STUDY ON THE BUBBLE BEHAVIOR AND ANODIC OVERVOLTAGE OF NiFe$_2$O$_4$ CERAMIC BASED INERT ANODES

Jinjing Du [a], Bin Wang[a], YihanLiu[b], GuangchunYao[b], Zhao Fang[a], Ping Hu[a]

[a]School of Metallurgy Engineering, Xi'an University of Architecture and Technology

[b]School of Materials and Metallurgy, Northeastern University

Key words: NiFe$_2$O$_4$ Ceramic, Inert Anodes, Bubble behavior, Anodic Overvoltage, Current Interruption Technique

Abstract

NiFe$_2$O$_4$ ceramic based inert anodes were fabricated by a two-step cold-pressing sintering process. The bubble behavior of NiFe$_2$O$_4$ ceramic based inert anodes was investigated in a two-compartment see-through quartz cell. Anodic overvoltage and potential decay curves on the inert anodes were measured by using the steady state and current interruption technique. The results show that the electrolytic gas evolution for NiFe$_2$O$_4$ inert anodes, including bubble nucleation, growth, coalescence, growth again, migration and escaping, lasts for 79s and the escaping bubble size is about of Φ4mm×2mm. While gas evolution lasts for 102s of carbon anodes with larger releasing bubbles. When current densities are 0.6, 0.8, 1.0 and 1.2A/cm^2, the anodic overvoltage of NiFe$_2$O$_4$ anodes are 0.189 V, 0.270 V, 0.309 V and 0.359 V, respectively. After adding small amount of MnO$_2$, V$_2$O$_5$, and TiO$_2$, a minor reduction in anodic overvoltage of NiFe$_2$O$_4$ anodes can be obtained.

Introduction

Much attention has been paid on novel techniques of aluminum electrolysis with inert anodes for many years [1, 2]. Current efficiency of aluminum electrolysis is 96% now, but consumable carbon anodes are used with product being CO$_2$, CO and fluorocarbons [3], which is an obstacle to economic development and environmentally friendly industrial production. Research on finding green materials as inert anodes has received much attention in the aluminum electrolysis industry. A patent applied by S. P. Ray in 1998 brought NiFe$_2$O$_4$ into researchers' view [4-6].Nickel ferrite (NiFe$_2$O$_4$) as one of the most important spinel ferrites, its cubic inverse spinel structure provides a better chemical stability in the molten cryolite-alumina bath [7-9]. Additionally, for its semiconducting characteristic, NiFe$_2$O$_4$ can be used as a promising candidate for green inert anodes. NiFe$_2$O$_4$ has attracted considerable attention for releasing environment-friendly O$_2$ gas during electrolysis instead of greenhouse gases.

Based on much literature, gas evolution on graphite and oxygen-evolving anodes, such as metal anodes and oxide anodes, was invested by polarization curve and other electrochemical methods. The current and potential response induced by anodic bubbles has been studied by Tie Jun et al. to figure out the bubble fluctuation on the surface of carbon anode [10]. Laurent Cassayre et al. [11] found that gas evolution was nearly identical for tin-oxide, copper, and copper-nickel anodes, but very different from what was observed on the graphite anode. The reaction mechanism of O$_2$ evolution on the IrO$_2$(x)+MnO$_2$(1-x) electrodes was studied by polarization curve [12]. The visual behavior of bubble evolved from metal anode was researched by Xu Junli to find the relationship between current density and bubble behavior [13]. However, more studies were focused on adjusting the composition and optimizing structure to obtain excellent performance for NiFe$_2$O$_4$inert anodes, just few on bubble behavior and anodic overvoltage, as well as other electrochemical performance of NiFe$_2$O$_4$ ceramic based inert anodes during electrolysis process [14-15], which was very important to evaluate its overall performance.

For this mentioned above, our work aims at more vividly depicting the dynamic bubble evolution from NiFe$_2$O$_4$ ceramic of anodes, figuring out how the wettability of molten electrolyte on NiFe$_2$O$_4$-based inert anode affects bubble evolution, and providing some convictive advice for modification of anodic overvoltage for NiFe$_2$O$_4$ ceramic based inert anodes with small amount of additives (such as MnO$_2$, V$_2$O$_5$, andTiO$_2$). For this purpose, the bubble behavior and anodic overvoltage of NiFe$_2$O$_4$ ceramic based inert anodes was investigated.

Experimental procedure

Synthesis

Samples of NiFe$_2$O$_4$ ceramic inert anodes were made from a mixture of NiO and Fe$_2$O$_3$ commercial powder. Early research has shown that a small amount of additive (MnO$_2$, V$_2$O$_5$, TiO$_2$) is in favor of obtaining good structural stability and excellent performance of NiFe$_2$O$_4$ ceramics, and the optimum adding level of MnO$_2$, V$_2$O$_5$, TiO$_2$ is 1.0 wt%, 0.5 wt%, and 2.5 wt%, respectively [16-18]. To analyze the effect of the three dopants on bubble evolution and electrochemical property of NiFe$_2$O$_4$ ceramic inert anodes, the doped samples with the three adding levels mentioned above were also prepared here. NiO and Fe$_2$O$_3$, with molar ratio 1.87:1, were mixed in planetary miller for 4 h using distilled water as dispersant, and dried completely in an oven. The dry powders with 4 wt% PVA binder turned to a set of blocks by cold-pressing molding under 60 MPa, transformed into the NiFe$_2$O$_4$ spinel matrix material after calcining at 1000°C in air for 6 h, and were crushed into powders again. Then the similar process was repeated: homogeneously mixing the mixture in the planetary miller for 4 h with distilled water as dispersant, drying the powders, molding the powers adding with 4 wt% PVA binder into green bodies by cold pressing with 200MPa. The green bodies were pre-fired at 450°C for 1 h to remove the PVA binder, and then sintered at 1200°C in air for 6 h to produceNiFe$_2$O$_4$-based inert anodes.

Wettability test

The surface of the prepared ceramic substrate for wetting tests was polished to the 0.5μm diamond paste level and cleaned ultrasonically, then blown dry. For deep comparative analysis of electrolyte affecting on NiFe$_2$O$_4$-based inert anodes and carbon anodes, a similar polishing process for the surface of carbon anodes was repeated. The electrolyte (Na$_3$AlF$_6$ +3wt% CaF$_2$+5wt% Al$_2$O$_3$) with NaF/AlF$_3$ molar ratio of 2.1 was

used. Sessile drop experiments were performed in an apparatus described in detail previously [19]. Wetting tests were conducted in a temperature range from 960°C to 1000°C. An amount of electrolyte like 0.2 ~ 0.3 gram were placed at the cleaned $NiFe_2O_4$ substrates and inserted in the hot zone of the furnace. As soon as electrolyte melted to form droplet on the $NiFe_2O_4$ substrates or carbon anode surface, a photograph was taken with a digital camera (7 million pixels model ESE-220c, Shenyang) and defined as the drop profile at zero time. Subsequent photos were taken at specific time intervals. Contact angles were measured directly from the captured photographs.

Visualization observation on anodic bubbles

Direct observation of electrolysis was carried out in a two-compartment see-through quartz cell (105mm × 70 mm × 100 mm) with the wall thickness of 3 mm, as shown in Figure 1. The quartz cell was divided into an anode chamber (70 mm in length) and a cathode chamber (35 mm in length) by a quartz baffle, a 1 mm slit was left at the bottom of the quartz baffle. The electrolytic experiments in two-compartment see-through quartz cell were conducted at a temperature of ~ 980 °C. In this see-through cell, the cathode was a graphite block (50 mm × 50 mm × 10 mm) located at the bottom of the cell, and the anode was either a graphite block (50 mm × 50 mm × 10 mm) or $NiFe_2O_4$-based inert anodes (cylinder, Φ=30mm, h=30mm), vertically positioned above the cathode. High-speed cameras (100 frames per second) and video cameras (24 frames per second) were adopted to observe all the electrolytic process, and record the bubble behavior. A new quartz cell was used for each experiment.
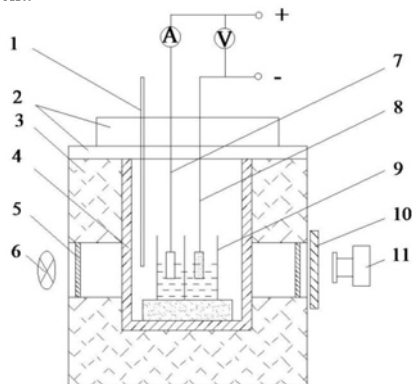

Figure 1. Two-compartment see-through Quartz electrolysis cell (105 mm × 70 mm × 100mm)
1-Thermocouple; 2-Capping; 3, 4-Side wall; 5-Glass;
6-Illuminant; 7-Anode;
8-Cathode; 9-Transparent quartz window; 10-Protection plate;
11-Camera

Anodic overvoltage test

Anodic overvoltage test was conducted in graphite crucible (Φ_{in} = 40 mm, h = 140 mm) with current interrupt technique. The electrolyte had the same composition as that used in wettability test. The anode was either a graphite cylinder or $NiFe_2O_4$-based inert anode with the same dimension (Φ 10 mm × 20 mm), liquid aluminum as cathode, the electrode distance maintained at 4~4.5 cm, and electrolytic temperature was 980 °C.

Results and discussion

Wettability of electrolyte to anodes

Studying wettability of electrolyte on anodes was particularly significant, because it would influence the electrolysis process, including anodic bubble evolution. Wettability of electrolyte to carbon anodes and $NiFe_2O_4$-based inert anodes was studied through sessile drop experiments.

(a) Softened electrolyte   (b) Molten electrolyte

(c) Droplet shape of electrolyte after melting 8min

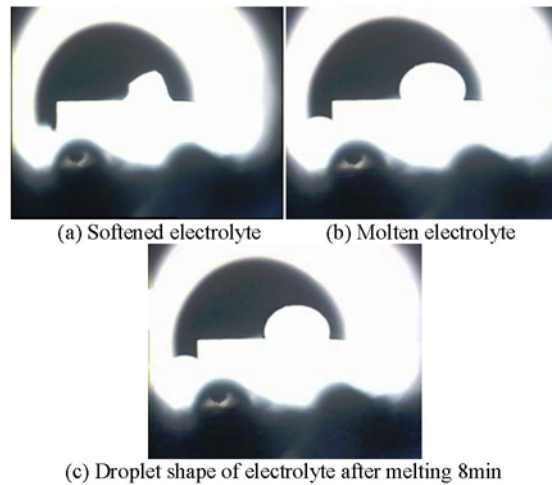Figure 2. Variation in wettability of electrolyte on carbon anode blocks.

It was observed that the initial wetting angle for the electrolyte (Na_3AlF_6 + 3wt% CaF_2 + 5wt% Al_2O_3) on carbon anodes was about 112.6°, as shown in Figure 3. As prolonging time, variation in wetting angles was not obvious. The contact angle of ~103.1° was obtained, when testing time last 12min.

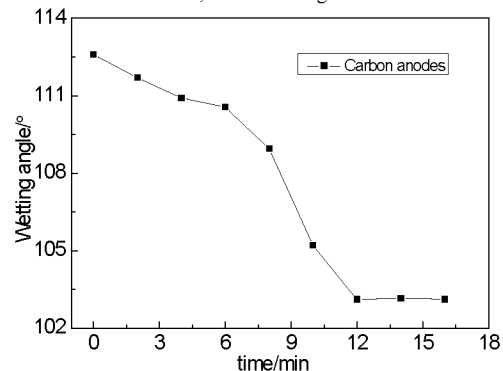Figure 3. Wetting angles versus time of carbon anodes.

The wetting process of electrolyte on the carbon anodes and $NiFe_2O_4$-basedinert anodes was shown in Figure 2 and Figure 4, respectively. It was found that the molten electrolyte converged into ellipsoid on the carbon anode firstly, then a relatively stable contact angle could be obtained. Figure 2 illustrated the wettability between carbon anode and electrolyte was not good (contact angle > 90°).

However, the wettability of electrolyte to $NiFe_2O_4$ anodes was quite different from that to carbon anodes. After completely melted, the electrolyte spread quickly on the $NiFe_2O_4$ substrate, and finally tended to be flattened on the contact surface of

NiFe$_2$O$_4$-based anodes. The electrolyte exhibited a better wettability on NiFe$_2$O$_4$ substrate than carbon anodes, which was indicated by Figure 4.

(a)Softened electrolyte   (b) Completely molten electrolyte
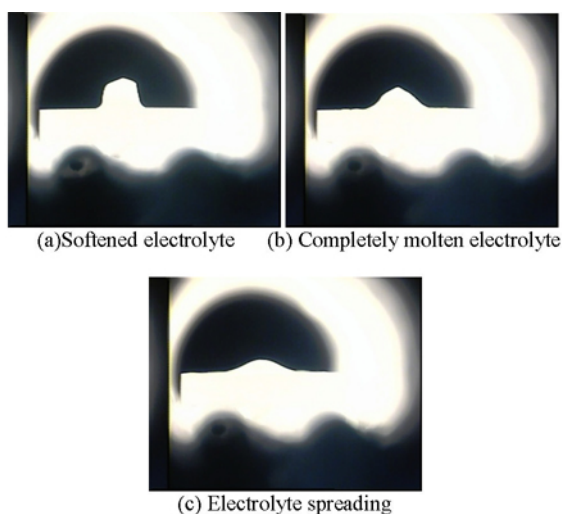

(c) Electrolyte spreading

Figure 4. Variation in wettability of electrolyte on NiFe$_2$O$_4$ blocks.

Through measurement and calculation, contact angle of 74.96°, 71.76°, 40.31° and 31.62° could be obtained, when testing time last 30 s, 60 s, 90 s and 120 s separately. As the molten electrolyte was flattened on the NiFe$_2$O$_4$ block, the wetting angle of 0°was unchanged.
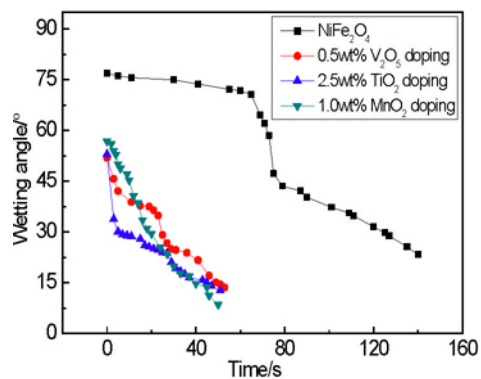

Figure 5. Wetting angles versus time of NiFe$_2$O$_4$-based anodes.

Additionally, influence of oxide additives (MnO$_2$, TiO$_2$, V$_2$O$_5$) on the wettability for electrolyte to NiFe$_2$O$_4$-based anodes was also taken into account. As shown in Figure 5, after introducing 1.0 wt% MnO$_2$, 2.5wt% TiO$_2$ and 0.5wt% V$_2$O$_5$ into NiFe$_2$O$_4$ substrate, the initial contact angle was 56.8°, 52.9° and 51.9°, separately. After testing 50s, the contact angle between electrolyte and NiFe$_2$O$_4$ substrate was less than 15°. To comprehensively concluded results, it could be regarded that the oxide additives could improve the wettability between the electrolyte and NiFe$_2$O$_4$-based inert anodes.

Anodic bubble evolution

Anodic bubble evolution is nearly identical for inert anode, but was found to be very different as compared to what was observed on the carbon anode. Observation of bubble growth process at the bottom of NiFe$_2$O$_4$-based anode showed tiny bubbles escaping continuously without much coalescence, forming a bubble at the bottom of the electrode, as illustrated in Figure 6. It could be seen that the bubble escaped with a diameter of 4 mm and ~2 mm in height, which is ten to 20 times smaller than that on carbon anode. The anodic bubble evolution process for NiFe$_2$O$_4$ anode, from bubble nucleation to escape lasted about 79 s, and the next evolution period started. However, for carbon anode, the bubble evolution period lasted about 102 s. It was also observed that the escaping bubble size for both carbon anode and NiFe$_2$O$_4$ anode decreased with increasing in current density, and the observations were difficult because the violent decomposition reaction of alumina happened with bubbles rapidly generating and escaping.
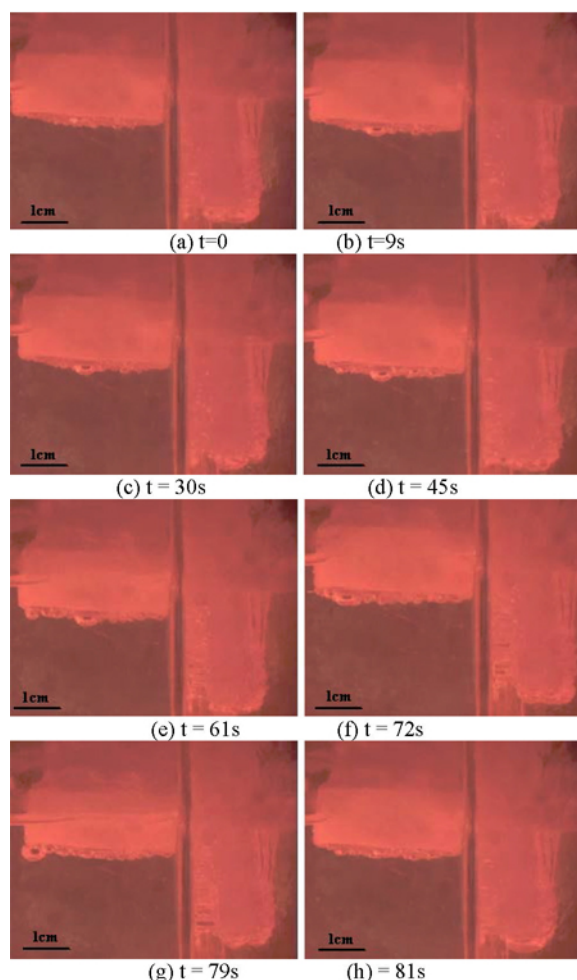

(a) t=0   (b) t=9s

(c) t = 30s   (d) t = 45s

(e) t = 61s   (f) t = 72s

(g) t = 79s   (h) = 81s

Figure 6. Bubble growth process at the bottom of NiFe$_2$O$_4$-based anodes.

Anodic overvoltage

Anodic overvoltage test was conducted with current interrupt technique and the interrupt current testing curves for carbon anodes and NiFe$_2$O$_4$ anodes were as shown in Figure 7 and Figure 8, respectively. It can be seen that the cell voltage of carbon anodes fluctuated violently comparing to that of NiFe$_2$O$_4$ anodes under the condition of different current density. For the both two anodes, severe fluctuation trend was illustrated with an
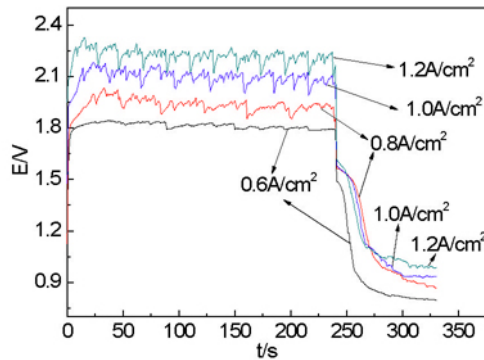
increase in current density.

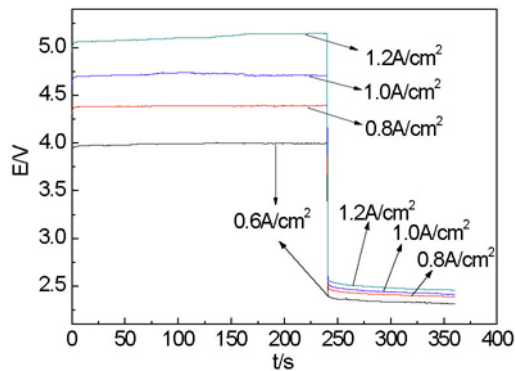Figure 7. Interrupt current testing curve of carbon anodes at 980 °C.

Figure 8.   Interrupt current testing curve of NiFe$_2$O$_4$ anodes at 980 °C.

It is known that overvoltage is equal to the back electromotive force (back-EMF) minus the theoretical decomposition voltage of carbon anode or NiFe$_2$O$_4$ anode. Back-EMF of anodes at 980°C under the condition of different current density could be obtained from the interrupt current testing curve directly. The theoretical decomposition voltage can be obtained by analyzing about thermodynamic data. Also, overvoltage consists of two parts: anodic overvoltage and cathodic overvoltage. Cathodic overvoltage of ~0.02 V is very small, which can be ignored. So, to some degree, anodic overvoltage is equal to back-EMF minus the theoretical decomposition voltage of carbon anode or NiFe$_2$O$_4$ anode. With analysis above, back-EMF and anodic overvoltage of carbon anodes and NiFe$_2$O$_4$ inert anodes at 980°C with different current densities were acquired, and the results as shown in Table 1.

Table 1. Back electromotive force and anodic overvoltage of carbon anodes and NiFe$_2$O$_4$ inert anodes at 980°C with different current densities.

		Current density(A/cm^2)			
	Anodes	0.6	0.8	1.0	1.2
back-EMF(V)	Carbon anode	1.48	1.56	1.58	1.61
	NiFe$_2$O$_4$anode	2.39	2.47	2.51	2.56
Anodic overvoltage (V)	Carbon anode	0.31	0.38	0.41	0.43
	NiFe$_2$O$_4$anode	0.18	0.27	0.31	0.35

Besides, the NiFe$_2$O$_4$ anode voltage with oxide additives as mentioned earlier, was measured during the electrolytic process.

After introducing 1.0 wt% MnO$_2$, 0.5 wt% V$_2$O$_5$ and 2.5 wt% TiO$_2$ into NiFe$_2$O$_4$ substrates separately, a slight decrease in the cell voltage, back-EMF and anodic overvoltage was observed during the electrolysis process. And the cell voltage was relatively stable. It was mainly due to improvement in wettability between electrolyte and NiFe$_2$O$_4$ substrate for introduction of the oxide additives.

Conclusion

The bubble behavior and anodic overvoltage of NiFe$_2$O$_4$ ceramic based inert anodes were investigated. The electrolyte exhibited a better wettability on NiFe$_2$O$_4$ substrate than carbon anodes. The oxide additives could improve the wettability between the electrolyte and NiFe$_2$O$_4$-based inert anodes. The electrolytic gas evolution for NiFe$_2$O$_4$ inert anodes, including bubble nucleation, growth, coalescence, growth again, migration and escaping, lasts for 79 s and the escaping bubble size is about of Φ4 mm × 2 mm. While gas evolution lasts for 102 s of carbon anodes with larger releasing bubbles the cell voltage of carbon anodes fluctuated violently comparing to that of NiFe$_2$O$_4$ anodes. After adding small amount of MnO$_2$, V$_2$O$_5$, and TiO$_2$, a minor reduction in anodic overvoltage of NiFe$_2$O$_4$ anodes could be obtained.

References

1. Y.Q. Lai et al., "Effect of Adding Methods of Metallic Phase on Microstructure and Thermal Shock Resistance of Ni/(90NiFe$_2$O$_4$-10NiO) Cermets", Transactions of Nonferrous Metals Society of China, 17(2007), 681-682.
2. J. Keniry, "The Economics of Inert Anodes and Wettable Cathodes for Aluminum Reduction Cells", JOM, 53(2001), 43-47.
3. J. Ma et al., "Research on Preparation and Properties of 18NiO-NiFe$_2$O$_4$ Composite Ceramic Inert Anodes", Light Metals, 2010, 949-952.
4. L.J. Berchmans et al., "Evaluation of Mg^{2+}-substituted NiFe$_2$O$_4$ as A Green Anode Material," Materials Letters, 58(2004), 1928-1933.
5. J.H. Yang et al., "The Behavior and Improvement of SnO$_2$-based Inert Anodes in Aluminum Electrolysis," Light Metals 1993, 493-495.
6. S. P. Ray, R. A. Rapp, "Composition Suitable for Use as Inert Electrode Having Good Electrical Conductivity and Mechanical Properties," US Patent: 4454015, 1984-02-08.
7. S. P. Ray, "Inert anodes for Hall cells". Light Metals 1986, 287-298.
8. E. Olsen, J. Thonstad, "Nickel Ferrite as Inert Anodes in Aluminium Electrolysis (part I): Material Fabrication and Preliminary Testing", Journal of Applied Electrochemistry, 29 (1999), 293-299.
9. D. R. Sadoway, "Inert Anodes for the Hall HároultCell: the Ultimate Materials Challenge",   JOM, 53 (2001), 34-35.
10. T. Jun, Z.Jiancheng, "On the Electrochemical Response of Anodic Bubbles in Aluminium Electrolysis", Computers and Applied Chemistry, 18(2001), 57-58.

11. L.Cassayre, T. A. Utigard, and Sylvie Bouvet, "Visualizing Gas Evolution on Graphite and Oxygen-Evolving Anodes", Journal of Minerals, Metals and Materials Society, 54(2002), 41-45.

12. Z.G. Ye, et al.,"Structure and Characteristics of $Ti/IrO_2(x)+MnO_2(1-x)$ Anode for Oxygen Evolution", Solid State Sciences, 10 (2008), 346-354.

13. J.L. Xu,etal.,"Bubble Behavior on Metal Anode of Aluminum Electrolysis," The Chinese Journal of Nonferrous Metals, 14 (2004), 298-301.

14. L.Cassayre, T. A. Utigard, and S. Bouvet, "Visualizing Gas Evolution on Graphite and Oxygen-evolving Anodes", JOM, 56 (2002), 41-45.

15. Q.Y. Li, et al., "Determination of Ohmic/Voltage Drop and Factors Influencing of Anodic Overvoltage of Carbon Anodes in Na_3AlF_6-Al_2O_3 based Melts", Transactions of Nonferrous Metals Society of China, 3 (2003), 699-703.

16. B. Wanget.al, "Effect of TiO_2 Doping on the Sintering Process, Mechanical and Magnetic Properties of $NiFe_2O_4$ Ferrite Ceramics", International Journal of Applied Ceramic Technology, Published online, DOI: 10.1111/ijac.12219, 2014.

17. J.J. Du,et.al, "Effect of MnO_2 Addition on Sintering Properties of $18NiO$-$NiFe_2O_4$ Composite Ceramics: Preliminary Results", Journal of Materials Engineering and Performance, 21 (2012), 1998-2001.

18. J.J. Du,et.al, "Influence of V_2O_5 as An Effective Dopant on the Sintering Behavior and Magnetic Properties of $NiFe_2O_4$ Ferrite Ceramics", Ceramics International, 38 (2012), 1707-1711.

19. D. W. Li, et.al, "Wetting Behavior of Al Alloys on A TiH_2 Substrate", Journal of Alloys and Compounds, 489 (2010), L1-L3.